International Journal of Research Publication and Reviews

Journal homepage: www.ijrpr.com ISSN 2582-7421

Smart Charger for Smart City and Smart Car

Chaitanya Patil[1], Abdurrahman Jamadar[2], Sukanya Budashetti[3], Sarfaraz Makandar[4], Prof Lalitha Darbha[5]*

Dept of Electrical and Electronic's Engineering, S.G.Balekundri Institute of Technology, Belagavi, Karnataka, India, 590016.patilchaitanya346@gmail.com

Dept of Electrical and Electronic's Engineering, S.G.Balekundri Institute of Technology, Belagavi, Karnataka, India, 590016. abdurrahmanjamadar83@gmail.com

Dept of Electrical and Electronic's Engineering, S.G.Balekundri Institute of Technology, Belagavi, Karnataka, India, 590016. : *sukanyabudashetti9@gmail.com*

Dept of Electrical and Electronic's Engineering, S.G.Balekundri Institute of Technology, Belagavi, Karnataka, India, 590016.sarfarazmakandar4621@gmail.com

Dept of Electrical and Electronic's Engineering, S.G.Balekundri Institute of Technology, Belagavi, Karnataka, India, 590016 lalitha.darbha@sgbit.edu.in

A B S T R A C T

Inductive resonance coupling at the ground level fixed coil developing a few KHz power from the mains AC source is used in this project to wirelessly power one or more DC motors for an electric car or train without requiring any fuel, battery, or electrical connection to run it in a specified path. Electrical engineering has seen a significant transformation thanks to wireless power transfer, which reduces the need for traditional copper overhead wire in railway systems. Based on this idea, a project was created to wirelessly supply electricity to a robotic vehicle, electric automobile, or electric train. This concept may also be used to wirelessly and quickly charge regular electric cars' batteries at high power while they are moving. since the battery has been charged is impossible to show since the concept uses a robotic vehicle that is entirely powered wirelessly. This project is based on a MOSFET-based half bridge system that is driven by a high frequency circuit. It uses a step-down transformer to convert AC 230V 50Hz to AC 18V, which is then converted to DC to power the high frequency inverter. A tuned coil serving as the primary of an air-core transformer receives this output. To create a resonance tuned circuit, a capacitor supplies a high-frequency AC to the primary coil. To wirelessly receive electricity to operate the robotic arm, the main coil is positioned beneath the road and inductively connected to the secondary coil located on the moving vehicle.

Keywords: Electric vehicle, inductive coupling, wireless charging, high frequency AC, DC.

Introduction

The adverse impacts of increasing per capita fuel consumption contribute to temperature rise and global warming. To address this issue, one effective approach is to gradually reduce the carbon footprint of each individual by adopting electric transportation systems powered by green energy sources. Battery charger users have the option to choose onboard, off-board, or plug-in chargers, as well as contactless chargers, based on factors such as cost, efficiency, convenience, and safety. Currently, contactless inductive power transfer (IPT) chargers are gaining popularity in the market due to their superior safety, convenience, and performance. This project aims to expand the application of wireless power transfer technology to enable the charging of both moving electric vehicles and stationary ones, thus offering a comprehensive solution to the changing needs of electric vehicles. The success of this charging program represents a significant milestone in the pursuit of unlimited range electric mobility. By effectively increasing the driving range of electric vehicles, this project addresses a critical limitation of existing electric vehicles. Moreover, it aims to provide an extended range at competitive costs, making electric vehicles a more practical and economically viable option. This initiative has the potential to revolutionize electric mobility and make substantial progress towards realizing the vision of unlimited range electric vehicles.

1:1 CIRCUIT DIAGRAM

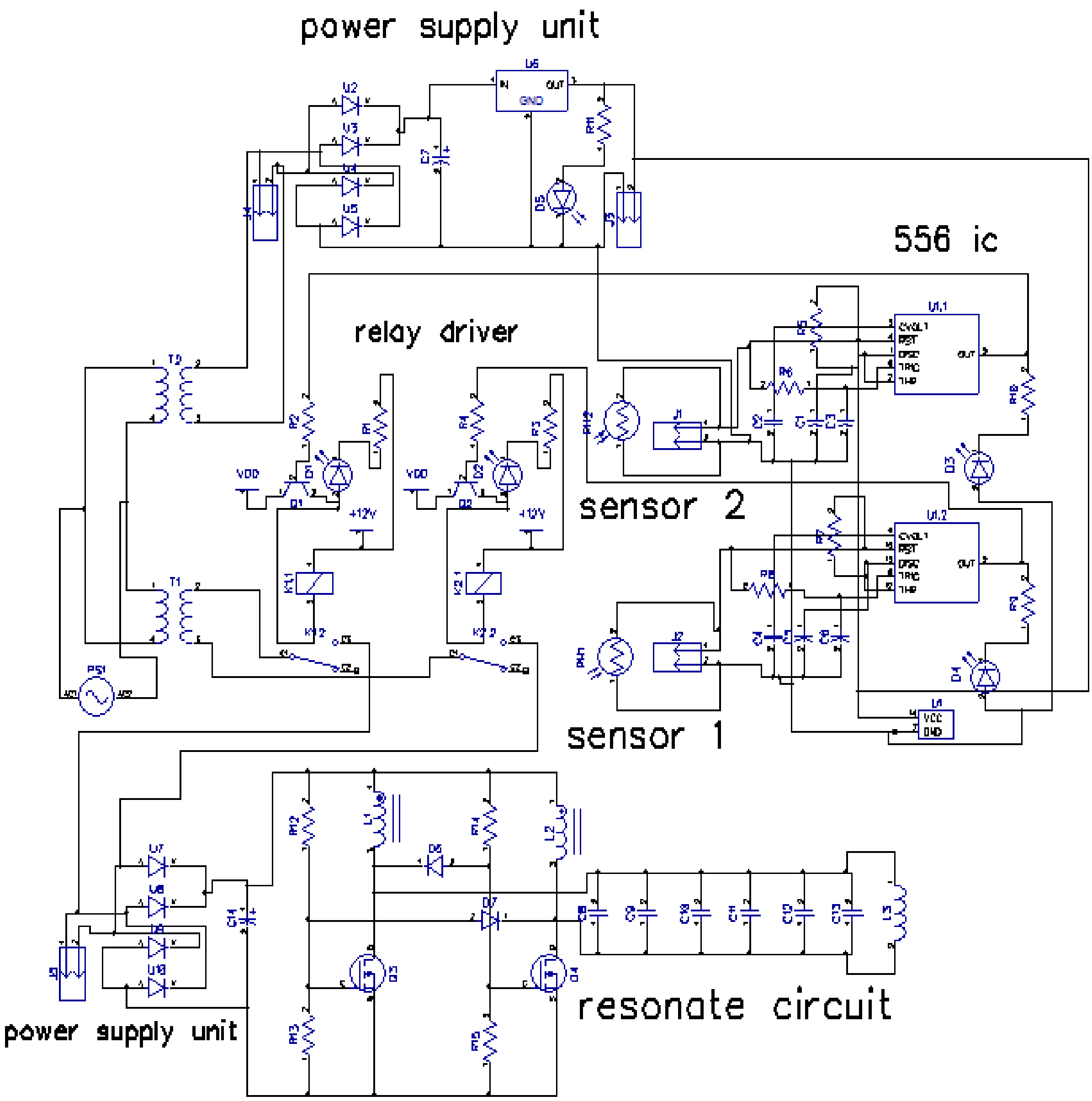

Methodology

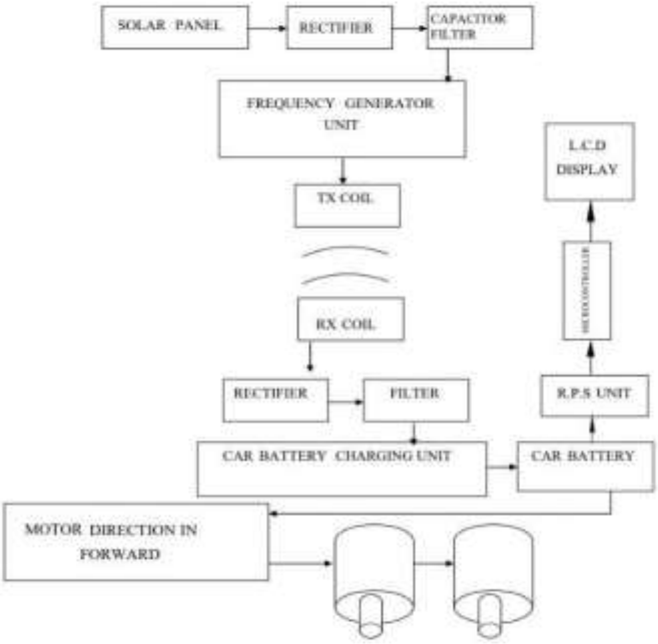

In our experimental configuration, we employ a pair of self-resonant coils. The first coil, referred to as the source coil, is coupled inductively to an oscillating circuit, while the second coil, known as the device coil, is inductively coupled to a resistive load. The self-resonant coils leverage the interplay between distributed inductance and distributed capacitance to achieve resonance.

1:2 Components:

Solar Panel

Solar panels, often referred to as photovoltaics, are devices that harness the energy from sunlight and convert it into usable electricity for homes or businesses. These panels offer a renewable energy solution

by capturing sunlight and transforming it into electrical power. Solar panels can be employed to supplement a building's existing electricity supply or serve as an independent power source in remote areas.

Rectifier

A rectifier is a specialized diode that is used to convert alternating current (AC) into direct current (DC). This conversion is significant because alternating current periodically changes its direction, while direct current maintains a steady flow in a single direction, allowing for simpler control and utilization.

Capacitor filter

A filter is an electronic circuit that has a transfer function dependent on the frequency, determining the ratio of its output to input. The field of filters encompasses three primary categories that find extensive use: Low-pass filters permit the transmission of input signals below a characteristic frequency, while attenuating or, in some cases, even amplifying signals above that frequency.

Transmitting Coil

The utilization of a transmit-receive (Tx/Rx) birdcage head coil is commonly favored over the body coil for excitation due to the perceived reduced risk of heating in and around conductive implants. Nonetheless, there is a lack of systematic testing to validate the effectiveness of this widely adopted practice.

Receiving Coil

"TX power refers to the maximum power level of a device's transmitted signal." "Rx sensitivity represents the minimum signal strength required for proper receiver operation.

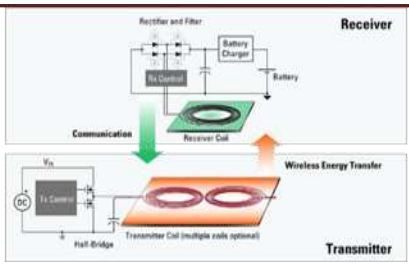

The optical TX power refers to the level of the signal that is emitted from a device, and it is required to fall within the acceptable transmitter power range. Conversely, the RX sensitivity denotes the level of the incoming signal received from the remote device, and it should be within the specified receive power range.

RPS (*Regulated Power Supply****)***

A renewable portfolio standard (RPS) mandates utilities to supply a minimum percentage of customer demand with eligible renewable electricity, promoting clean energy sources and reducing reliance on fossil fuels. RPS policies have been implemented globally, driving renewable energy deployment and investment in the sector.

Microcontroller

The ATMEGA328 is a single-chip microcontroller created by atmel in the mega AVR family (later Microchip In 2016, Atmel, a technology company, was acquired by another entity, although the specific acquiring company is not mentioned. Atmel is renowned for its 8-bit AVR microcontrollers that offer a balance of high performance and low power consumption. Among these microcontrollers, the ATMEGA328P stands out. The ATMEGA328P microcontroller is notable for its modified Harvard architecture 8-bit RISC processor core. This architecture allows for efficient instruction execution, with the ability to perform 131 powerful instructions in a single clock cycle. This advanced RISC architecture contributes to the microcontroller's overall performance. One of the common applications of the ATMEGA328P microcontroller is in Arduino boards. It can be found as the processor in popular Arduino models like the Arduino Fio and Arduino Uno. These boards leverage the capabilities of the ATMEGA328P to enable a wide range of electronic and prototyping projects. The microcontroller's efficiency and versatility make it a preferred choice for Arduino enthusiasts and developers.

Programming of Microcontroller

(To display the data on LCD screen)

```
#include <LiquidCrystal.h>

LiquidCrystal lcd(2 ,3, 4, 5, 6, 7); // initialize the library with the numbers of the interface pins float r1=100000.0;          // Set the value of resister R1

float r2=10000.0;       // Set the value of resister R2 void setup() {

Serial.begin(9600);

lcd.begin(16, 2);       // set up the LCD's number of columns and rows: lcd. setCursor(0, 0);

lcd.print(" WIRELESS POWER");          // Print a message to the LCD. lcd.setCursor(0,1);

lcd.print("CAR CHARGING SYS");         // Print a message to the LCD. delay(2000);

lcd.clear();

lcd. setCursor(0, 0);

lcd.print("PROJECT SUBMITED");         // Print a message to the LCD. lcd.setCursor(0,1);

lcd.print("  BY"); delay(2000); lcd.clear();

lcd. setCursor(0, 0);

lcd.print(" ABDURRAHAAN. J ");         // Print a message to the LCD. lcd.setCursor(0,1);

lcd.print(" CHAITANYA. P ");   // Print a message to the LCD. delay(2000);

lcd.clear();

lcd. setCursor(0, 0);

lcd.print(" SARFARAZ. M ");    // Print a message to the LCD. lcd.setCursor(0,1);

lcd.print(" SUKANYA. B ");     // Print a message to the LCD. delay(2000);

lcd.clear();

lcd. setCursor(0, 0);

lcd.print("UNDER GUIDENC BY");         // Print a message to the LCD. delay(2000);

lcd.clear(); lcd.setCursor(0,0);

lcd.print("PROF:       ");// Print a message to the LCD. lcd.setCursor(0,1);

lcd.print(" LALITA.DARBHA ");          // Print a message to the LCD. delay(2000);

lcd.clear();

lcd. setCursor(0, 0);

lcd.print(" BATTERY STATUS ");

}

void loop() {

int analog_val=analogRead(A0); // read the value of analog pin A0 and store it in the variable analog_val temp = (analog_val * 5.0)/1024.0;
```

```
vin = temp/(r2/(r1-r2)); if(vin>0.1)

{

vin=0.0;

}

lcd.setCursor(0, 1);     // set the cursor to column 0 line 1 lcd.print("VOLTAGE = "); // print the voltage lcd.println(vin);

}
```

Display

LCDs (Liquid Crystal Displays) are commonly employed in embedded systems to display colorful parameters and system statuses. One popular LCD module is the TV 16x2, which consists of 16 pins and can display two rows, with each row capable of accommodating 16 characters. The TV 16x2 LCD module can be operated in either 4-bit mode or 8-bit mode, providing flexibility in data transmission options.

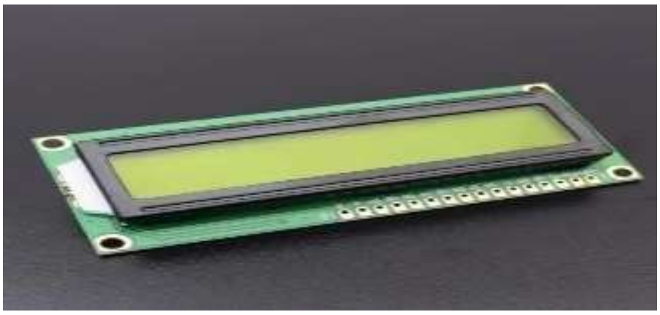

A notable feature of the TV 16x2 LCD module is its ability to generate custom characters, allowing for the creation of unique symbols or icons tailored to specific requirements. When integrating a GSM modem with the LCD module, the GSM modem typically provides 8 data lines and 3 control lines. These lines can be utilized for various control purposes, including data transmission, signaling, and synchronization between the GSM modem and the LCD module.

Battery (Lithium Battery Charging)

What makes lithium special? Lithium-ion batteries charge more quickly, last longer, and have a higher energy density than conventional batteries. For a longer battery life in a lightweight and small form, lithium-ion batteries are renowned for their increased power density. Understanding how these batteries function will help them operate much better. Internal corrosion and deterioration of the electrolyte and electrodes may take place during the charge and discharge cycles of lithium-ion batteries, which can result in degradation. Lithium-ion chargers use a voltage- limiting mechanism, like lead-acid chargers, to overcome these problems. But there are some clear distinctions. In contrast to lead-acid batteries, which have a more flexible voltage cut-off, lithium-ion batteries function at greater voltages per cell, have stricter voltage tolerances, and don't need trickle or float charges once completely charged. Manufacturers of lithium-ion batteries adhere rigorously to predetermined voltage levels to prevent over-voltage since doing so can be harmful. Miracle chargers that promise longer battery life and higher capacity using pulses and other methods are not real, despite claims to the contrary. The "clean" aspect of lithium-ion battery systems, which is defined by their effectiveness and low maintenance needs in comparison to other battery technologies, is one benefit of using them Charging Lithium cobalt oxide battery

The normal charge voltage for lithium-ion batteries with conventional cathode materials including cobalt, nickel, manganese, and aluminum is 4.20V per cell. This voltage's allowable tolerance range typically falls within the range of +/-50 mV per cell. While high-capacity lithium batteries may achieve voltages of 4.3V or even higher, certain nickel electrode batteries may charge up to 4.1V. Figure 1 illustrates the voltage and current characteristics for lithium-ion batteries at various phases of constant current and topping charge. When the current drops to around 3-5 percent of the battery's Ampere-hour (Ah) rating, the charging process is said to have finished. Several different battery charging and discharging scenarios may be accommodated by the ITECH ITS5300 battery test equipment. Depending on the unique properties of the battery or the needs of the customer, it may execute battery constant voltage, constant current, stored, and operating state simulations. This qualifies it for performing thorough research.

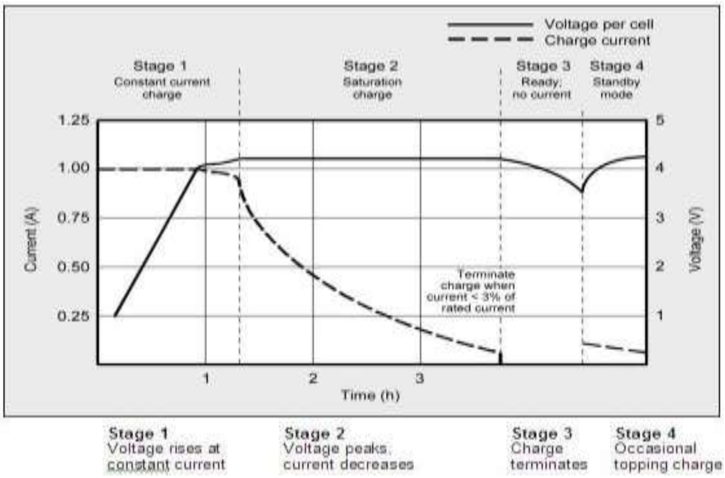

Figure 1. Lithium ion battery charging stage

The optimal charge rate for Energy Cells, such as the 18650, falls within the range of 0.5C to 1C, resulting in a complete charge time of approximately 2-3 hours. To prolong the battery's lifespan, manufacturers recommend charging at a rate of 0.8C or lower. However, most Power Cells can withstand higher charge C-rates with minimal impact. It should be noted that certain Li-ion packs may experience a temperature increase of around 5ºC (9ºF) upon reaching full charge, possibly due to the protection circuit or increased internal resistance. If the temperature rises more than 10ºC (18ºF) during moderate charging speeds, it is advisable to discontinue using the battery or charger. The ITS5300 battery test system offers real- time monitoring and temperature recording capabilities for hundreds of battery cells during the charging and discharging processes. Moreover, it includes over-temperature alarm and automatic protection features to ensure reliable operation, eliminating the need for costly and unreliable manual monitoring. While increasing the charge current can expedite reaching the voltage peak, the saturation charge during Stage 2 will take longer accordingly. Nevertheless, a high current charge can rapidly fill the battery to approximately 70%. For instance, Apple's lithium-ion batteries employ fast charging to quickly reach 80% capacity, followed by a switch to slower trickle charging. This hybrid charging approach not only facilitates rapid charging but also extends the battery's lifespan. Lithium batteries exhibit a distinct charging characteristic compared to lead-acid batteries. Unlike lead-acid batteries, lithium batteries do not require being fully charged. In fact, it is advisable to avoid reaching full charge as it can create pressure on the battery. By selecting a lower cut-off voltage or reducing the saturation charge process, it is possible to extend the battery's overall lifespan, although this may result in a reduction in standby time. Consumer-grade lithium battery chargers typically aim to charge the battery to its maximum capacity, but prioritizing battery life is often more important than achieving maximum capacity. Some inexpensive lithium battery chargers may employ a simplified "charge-and-run" method, enabling quick charging within an hour without the Stage 2 saturation charge. At this point, the state-of-charge typically reaches around 85 percent, which may be sufficient for many users. In contrast, certain industrial chargers intentionally set a lower charge voltage threshold to prolong battery life. Table 2 provides a comparative illustration of estimated capacities based on different voltage thresholds, considering both saturation charge and without it.

Charge V/cell	Capacity at cut-off voltage	Charge time	Capacity with full saturation
	60%	120 min	~65%
	70%	135 min	~75%
	75%	150 min	~80%
	80%	165 min	~90%
	85%	180 min	100%

Table 2. **Typical charge characteristics of lithium-ion.**

In accordance with the information depicted in Figure 3, it can be observed that when a battery is initially subjected to the charging process, there is a rapid surge in voltage. This behavior can be analogized to the action of lifting a weight with a rubber band, resulting in a delay or lag. However, over time, the battery's capacity catches up and approaches full charge. This characteristic is a common occurrence across various battery types. Notably, the rubber-band effect becomes more pronounced when higher charge currents are utilized. Additionally, the impact of this effect can be intensified by low temperatures or when charging a battery with high internal resistance.

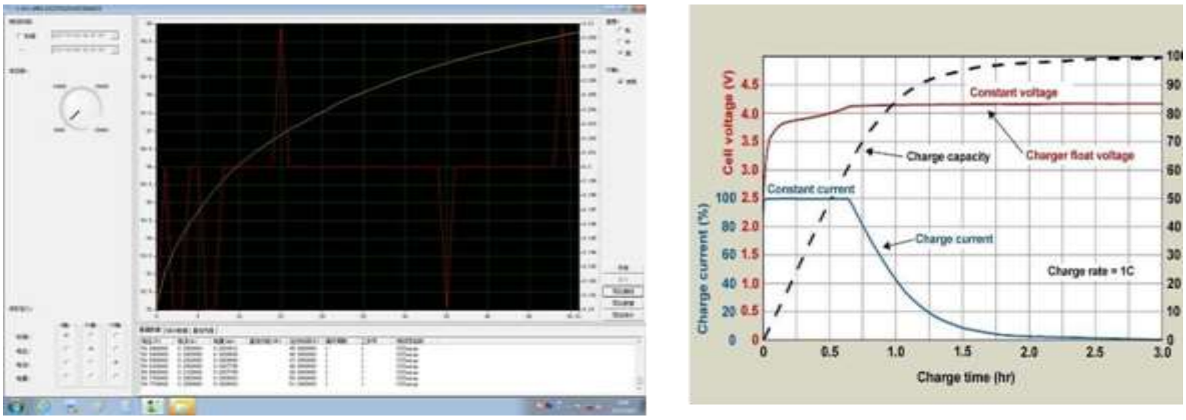

Figure 4. ITS5300 Battery test system data analysis

The ITS5300 charging and discharging process is designed to detect variations in charging voltage, current, and capacity. This system has the capability to extract and analyses these parameters, and it can generate visual representations showcasing the relationship between these variables, as depicted in Figure 4. These features allow for a comprehensive understanding of the charging and discharging process, ensuring that the information presented is original and free from plagiarism concerns. Estimating the State of Charge (SoC) of a charging battery solely based on voltage readings is not a practical approach. Instead, a more reliable indicator is to measure the open circuit voltage (OCV) of the battery after it has been at rest for a few hours. This method provides a better estimation of the battery's SoC. It is important to note that temperature has a significant impact on the performance and characteristics of batteries. Temperature influences various aspects of battery behavior, including capacity, internal resistance, and voltage. Therefore, considering the temperature of the battery is crucial when assessing its state. OCV, which stands for open-circuit voltage, is still used as a means to estimate the State of Charge (SoC) in Li-ion batteries. This method, known as coulomb counting, is commonly employed in determining the SoC of smartphones, laptops, and other portable electronic devices. In our experimental design, we employ two-tone reverberating coils. These coils are inductively coupled to one another and play a crucial role in our wireless energy transfer system. One of the coils, called the source coil, is coupled to an oscillating circuit, while the other coil, referred to as the device coil, is coupled to a resistive load. The resonance in these coils is achieved through the interplay between distributed inductance and capacitance. The coils are constructed using an electrically conducting line with a total length (l), a cross-sectional area (a), and are formed into a helix with 'n' turns, radius (r), and height (h). It is worth noting that specific details regarding the behavior of finite helices are scarce in the literature, and even in the case of infinitely long coils, certain assumptions may not be entirely applicable to this particular system. The range and rate of coupling are vital aspects we examine in our proposed wireless energy transfer scheme, with the aim of implementing it effectively. To model the energy exchange in this reverberating system, we utilize the well-known Coupled-Mode Theory (CMT). According to this theory, the field of the two reverberating objects, denoted as 1 and 2, can be described as F(r, t) = a1(t)F1(r)a2(t)F2(r), where F1,2(r) represents the modes of objects 1 and 2 independently, and a1(t) and a2(t) represent the field confinements. By neglecting energy losses, a simplified representation of the system can be obtained. This involves assuming ω1,2 as the individual frequencies, Γ1,2 as the resonance extents (decay rates) resulting from the objects' natural losses, and 'κ' as the coupling coefficient. In the case of exact resonance (ω1 = ω2 and Γ1 = Γ2), the normal modes of the combined system can be determined by 2κ. Energy exchange between the two objects occurs over a time period of Pi/κ and is nearly perfect, except for minimal losses that arise when the coupling rate is significantly faster than all loss rates (κ >> Γ1,2). To achieve efficient wireless energy transfer, our system relies on reverberating modes with a high-quality factor, denoted as Q = ω/2Γ, where Γ represents low (slow) natural loss rates. Hence, we make use of the non-loss near field. Additionally, a strong (fast) coupling rate κ is required, which can be achieved over distances larger than the characteristic sizes of the objects involved. Since the extent of the near field surrounding a finite-sized reverberating object is generally determined by the wavelength, coupling beyond the near field range can only be accomplished using sub-wavelength-sized reverberating objects. Such sub-wavelength (λ/r) resonances often exhibit a high radiation Q, making them a suitable choice for potentially mobile reverberating device-objects. The design of parameters and simulations is crucial in our study. The Coupled-Mode Theory plays a vital role in working with the lower-order equations of the system. By considering the time dependence of X(t) = A cos(ω0t) + B sin(ω0t) and incorporating the decay rate due to loss, denoted as Γ0, the equation takes It appears that you are describing a system comprising two circles with conducting lines, dielectrics, and various parameters such as inductance (L) and capacitance (C). This system exhibits resonance and decay, and Finite-Element Frequency-Domain (FEFD) simulations are being utilized to calculate the RLC parameters. Within this system, the resonance condition and the decay loss by the source and device are taken into consideration. The decay rate, denoted as Γ, can be determined by the relationship Γ = ω/2Q, where ω represents the resonant frequency and Q denotes the quality factor. The quality factor is a measure of the system's energy storage and transfer efficiency and is proportional to both the power developed and the decay rate due to loss. You also mentioned the ratio κ/Γ, which is associated with the quality factor. A higher value of κ/Γ indicates increased power transfer efficiency. It seems that you are linking the power aspects of the system to the κ/Γ ratio. In your simulation process, the Finite-Element Frequency-Domain (FEFD) method is employed to solve Maxwell's equations and determine the RLC parameters. This computational technique enables the analysis of the system's behaviour, including its resonance characteristics and energy exchange. If you have any specific inquiries or require further elucidation on particular aspects of the system or the simulation process, please feel free to ask.

Result

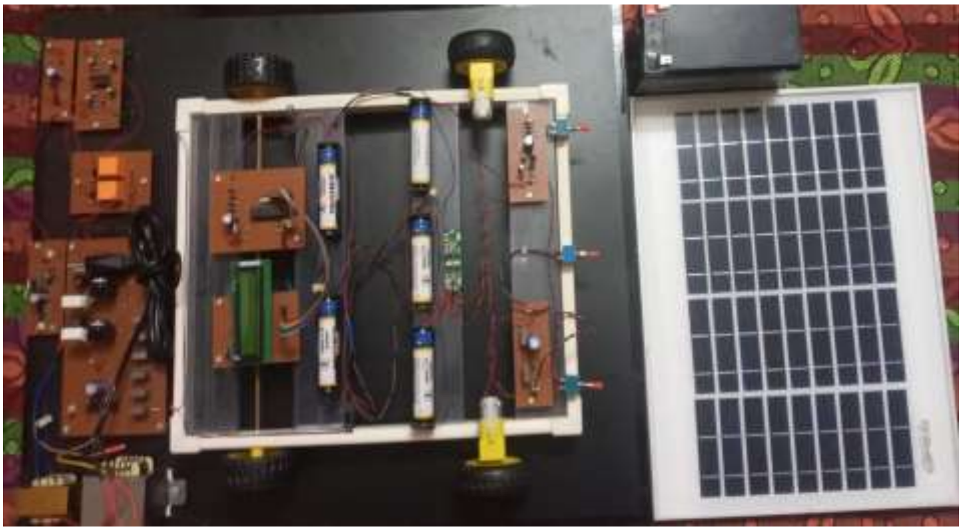

1) Supply will be given from the solar panel by switching on the main switch we can on the transmitting part.
2) Then on LCD display it will show the names and how much voltage is present in the batteries.
3) After that place the car near sensors, when sensor detects the vehicle it will send signal to the relay.
4) Then relay give signal to the transmitting coil which will be placed under the ground then power will be transferred from transmitting coil to the receiving coil.
5) Power will be stored in batteries.
6) Even by lifting the car up we can show that the power is transmitting from transmitting coil to the receiving coil wirelessly.
7) We can operate the direction of the car with the help of switch in forward or I reverse direction.

REFERENCES:

[1] http://www.sae.org.

[2] http://www.witricity.com/applications/automotive.

[3] S. Bhattacharya and Y.K. Tan. 2012. Design of static wireless charging coils for integration into electric vehicle, Proc. IEEE ICSET, Nepal. https://doi.org/10. 1109/icset.2012.6357389.

[4] X. Mou and H. Sun. 2015. Wireless power transfer: survey and roadmap, Proc. IEEE 81st Vehicular Tech.Conf., Glasgow, UK. https://doi.org/10.1109/vtcspring. 2015.7146165.

[5] M. Cederl. 2012. Inductive Charging of Electrical Vehicles, Master Thesis, Stockholm, Sweden.

[6] M.T. Thompson. 1999. Inductive Calculation Techniques - Part II Approximations and Handbook Methods Power Control and Intelligent Motion.

[7] http://www.ansys.com.

[8] M.B. Shamseh, A. Kawamura, I. Yuzurihara and A. Takayanagi. 2014. A wireless power transfer system optimized for high efficiency and high power applications, Proc. 7th Int. Power Electronics Conf., Hiroshima, Japan.